International Journal of Robotics and Control Systems
Vol. 4, No. 2, 2024, pp. 779-794
ISSN 2775-2658
http://pubs2.ascee.org/index.php/ijrcs

Power Regulation of a Three-Phase L-Filtered Grid-Connected Inverter Considering Uncertain Grid Impedance Using Robust Control

Socheat Yay [a,b,1], Panha Soth [a,2], Heng Tang [a,3], Horchhong Cheng [a,4], Sovann Ang [c,5], Chivon Choeung [a,6,*]

[a] Faculty of Electricity, National Polytechnic Institute of Cambodia, Phnom Penh, 120901, Cambodia
[b] Graduate School, National Polytechnic Institute of Cambodia, Phnom Penh, 120901, Cambodia
[c] Transmission Department, Electricity of Cambodia, Phnom Penh, 120405, Cambodia
[1] yaysocheat@npic.edu.kh; [2] sothpanha@npic.edu.kh; [3] tangheng@npic.edu.kh; [4] horchhong@gmail.com; [5] ang.sovann77@gmail.com; [6] choeungchivon@npic.edu.kh
* Corresponding Author

ARTICLE INFO

Article history
Received April 10, 2024
Revised May 14, 2024
Accepted May 25, 2024

Keywords
Grid-Connected Mode;
Linear Matrix Inequality;
Robust Control;
Uncertainty;
L-Filter

ABSTRACT

Uncertain grid impedance is often common in power distribution networks; therefore, it is crucial to design an efficient controller in this situation. An issue that frequently occurs is the problem of unpredictable grid impedance, which can cause voltage fluctuations, power quality problems, and potential damage to equipment. This work provides a systematic control strategy to tackle these issues by supplying well-regulated power from a DC source to an AC power grid. A linear matrix inequality (LMI)-based robust optimal control is proposed in this paper to provide stability to the inverter system without offset error at the output side. The convergence time to steady state is minimized by solving the LMI problem to maximize the eigen value of the closed-loop system with the inclusion of the uncertainty of the filter parameter and grid impedance. Furthermore, the uncertainties in this study include the potential variation of values for the filters and the grid's impedance. These uncertainties occur because the grid impedance can fluctuate fast in the event of a fault or termination of a transmission line, while the filter's impedance can also be affected by changes in operating temperature. The simulation study of this proposed control includes a comparison between wide and narrow uncertainty ranges, as well as a performance comparison under uncertain parameters. Furthermore, this approach exhibits a lower power ripple in comparison to existing PI control method.

1. Introduction

Renewable energy systems rely heavily on three-phase grid-connected inverters. They are in charge of converting the DC power produced by renewable energy sources like wind or solar panels into AC power that the grid can use [1]. As a result, renewable energy sources may be more easily integrated into the grid while cutting down on emissions of greenhouse gases and reducing the dependence on fossil fuels. A steady and dependable supply of power from renewable sources may be assured with the help of three-phase grid-connected inverters, which enable efficient power

transmission and distribution. Thus, grid-connected inverters are crucial to a sustainable and resilient energy system [2]. Grid impedance is the combined measure of resistance and reactance in the electrical grid, which acts as a constraint on the current flow in a power system. Understanding grid impedance is vital in power systems since it directly impacts the stability, dependability, and effectiveness of the system. An issue that frequently occurs is the problem of unpredictable grid impedance, which can cause voltage fluctuations, power quality problems, and potential damage to equipment. To effectively tackle this issue, it is necessary to employ precise modeling and continuous monitoring of grid impedance in order to guarantee optimal control and functioning of the power system. In recent years, the primary research objectives have been centered around controlling three-phase inverters in order to achieve optimal efficiency and robust performance.

Deadbeat control is a control strategy that seeks to provide a rapid and accurate response in a system. An extensive review [3] provided a comprehensive analysis of deadbeat current control (DBCC) in grid-connected inverters. The evaluation explored research findings, various deadbeat control methodologies, concerns regarding stability, and the challenges associated with its implementation. In [4], a method was proposed to regulate inverters by using improved deadbeat control. This approach aims to address issues including sluggish dynamic response and current harmonic disturbances in three-phase LCL grid-connected inverters. The current inner loop utilizes fuzzy PI for voltage control, discrete QPR for current control, and enhanced deadbeat control. The approach described in [5] utilized adaptive control to achieve a near-deadbeat response on a three-phase grid-connected inverter with an RL filter. This was accomplished by employing a parameter estimate architecture in a synchronous frame of reference. This method facilitated real-time modification of controller parameters to optimize performance. Most of these methods provide fast transient response and cancel out the external disturbances that may affect the system. Deadbeat control provides several advantages, such as enhanced system performance and stability. It guarantees quicker response times, minimizes steady-state error, and improves disturbance rejection capabilities. In addition, deadbeat control efficiently reduces overshoot and settling time, resulting in enhanced accuracy and precision in control. However deadbeat control has downsides. It is prone to parameter variations and uncertainties since it relies on accurate system models and estimations. Deadbeat control may not work for complex systems or those that need constant control. In such instances, different systems of control may work.

Model predictive control (MPC) is a commonly employed control approach in diverse industries for optimizing the performance of dynamic systems. Predictive control is a technique that use a mathematical model of a system to anticipate its future behavior and make control decisions based on those predictions. Advancements have been made to enhance the control precision and resilience of MPC methods used in three-phase grid-connected inverters. Researchers have suggested an enhanced MPC system that utilizes a disturbance observer to tackle power quality problems [6]. In addition, researchers have investigated the application of Finite Control Set Model Predictive Control (FCS-MPC) in a three-phase, three-level voltage source inverter to enhance convergence and precision of control [7]. Event-triggered MPC methods have also been developed for three-phase grid-connected inverters, where control actions are triggered only when state errors exceed a preset threshold [8]. Furthermore, the integration of FCS-MPC with a direct PQ control scheme has been investigated to achieve high-performance decoupled active and reactive power control in grid-tied inverters [9]. The implementation of virtual synchronous generator techniques in current-source inverters in multivariable MPC aims to regulate grid frequency and minimize distortions in grid current [10]. In addition, in order to comply with military regulations and reduce the occurrence of common mode conducted emissions, three-phase, four-wire grid-connected inverters have implemented innovative approaches such common mode voltage reduction techniques [11]. In addition, grid-connected systems have suggested the use of sliding mode-based FCS-MPC for bidirectional power inverters in order to assist microgrids by injecting or requesting energy from the AC grid [12]. The approach proposed in [13] utilizes the Kalman filter to eliminate the need for the system model. This method enhances the ability to precisely track the grid current and enhances its capacity to respond to changes in parameters, even when there is a mismatch. In addition to MPC, [14] introduced an event-triggered model predictive control approach for inverters, which enables

the connection of DC microgrids with battery-supercapacitor hybrid energy storage systems to the grid. This system has the potential to greatly decrease the number of control activities by removing superfluous procedures. Nevertheless, MPC is recognized for its limitations, which encompass complicated mathematical models, demanding computational power, and the necessity for precise system identification. In the absence of integral control or disturbance observer, the system's output may exhibit an offset error.

Direct power control (DPC) is a control approach used in grid-connected inverters to directly regulate both real and reactive power, eliminating the need for a separate current control loop. This technology is widely employed in renewable energy systems, including photovoltaic and wind power systems. DPC provides benefits such as rapid and precise power regulation, enhanced system stability, and less intricacy in comparison to conventional control techniques. A modified Maximum Power Point Tracking (MPPT) algorithm has been introduced in [15], which utilizes power perturbation instead of voltage or current perturbation to enhance the speed of the dynamic reaction. This approach offers a rapid and responsive transient while maintaining an acceptable steady-state performance by eliminating any internal control loops or interface variables. A comprehensive DPC method is introduced in [16] for a nine-level inverter connected to a power grid. The findings of this approach demonstrate that the inverter effectively produces the desired levels of active and reactive power while maintaining a standard level of Total Harmonic Distortion and ripple in the DC voltage. A novel control technique has been proposed in , which utilizes DPC with virtual flux to mitigate the adverse effects caused by disturbances in the power grid on grid-connected converters. Subsequently, [17] proposed a DPC method that relies on instantaneous power theory and employs optimized PI controllers through the utilization of a grey wolf optimizer (GWO) algorithm. Method discussed in [18] analyzed different reactive power control techniques for photovoltaic micro-inverters, while [19] proposed a model predictive DPC for a grid-interlinking converter of a battery energy storage system, which was helped by fuzzy decision-making. These methods emphasize several control systems and technologies that target enhancing the performance and efficiency of three-phase grid-connected inverters. However, there is one significant drawback of common DPC is high sampling frequency to reduce current ripple.

Utilizing PI control [20], which brings together proportional and integral control, provides numerous advantages in grid-connected inverters. It guarantees precise and accurate control of power output, reducing errors and enhancing the overall efficiency of the system. Power control using PI has been proposed in [21] for a grid-connected inverter under unsymmetrical system. Where [22] discussed a new PI method based on feed-forward for a three-phase grid-connected inverter. The study of [23] centered on regulating the DC voltage of boost converters in wind turbine systems by employing a PI controller. Similarly, [24] introduced a hybrid-frequency parallel inverter system that is coupled to a three-phase four-wire grid. The system incorporates ripple improvement to provide both minimal current distortion and fast response. Furthermore, [25] did a study on sophisticated current control algorithms for three-phase grid-connected PWM inverters used in distributed generating. In, a method for monitoring and controlling DC voltage in three-phase grid-connected wind turbine inverters has been proposed. Using a similar approach, [26] applied a space vector pulse width modulation (SVPWM) current controller to a three-phase grid-connected photovoltaic system. The article presents a discussion on the comparison of PI and fuzzy-logic controllers for three-phase grid-connected solar systems. Later, [27] focused on managing circulating currents in parallel grid-connected three-phase inverters. A PI inverter controller for a grid-connected PV system has been proposed in [28] using a particle swarm optimization technique. The aim was to improve the power quality performance. These abovementioned studies highlight the performance and effectiveness of PI control in terms of achieving precise voltage and frequency regulation. Moving forward, potential future developments and improvements in PI control can further enhance the performance and reliability of grid-connected inverters. However, it is important to note that PI control also has its limitations, such as the complexity of implementation and the need for proper tuning to achieve optimal performance.

It is important to emphasize that the approaches discussed in the literature do not consider uncertain grid impedance, which is crucial for ensuring stability and robustness in control design. To address some of the shortcomings of the previous methods, this paper proposes a systematic control design for a three-phase grid-connected inverter with the inclusion uncertain grid impedance. Unlike MPC or DPC, this control requires less computational power and a sampling frequency of just 10 kHz. The rationale for this is that the proposed approach eliminates the need to solve an optimization problem at each time step in order to obtain the optimal control inputs for the system. Only one solution to the LMI-based optimization problem is needed, and the stabilizing gain can be used without any further changes. In addition, this proposed robust control not only considers the uncertain parameters of the system but also the uncertain impedance of the grid side to provide more resilient performance to the inverter system, which is difficult to obtain using deadbeat control. Furthermore, due to the simplicity of the process to obtain robust gain, this method effortlessly provides optimal output power to the grid, unlike PI control. To verify the efficacy of this control method, various simulations have been conducted under variations in system and grid impedance. The simulation analysis in this paper was conducted using MATLAB to calculate the optimal gain, with assistance from the YALMIPS toolbox. Subsequently, the calculated robust gain is employed in the implementation of the control method in PSIM. Furthermore, the performance comparison between the PI control is also done to confirm the superiority of this proposed control. The simulation confirms that the proposed control exhibits a lower level of active power ripple (1.25%) in comparison to the PI control (7.25%), as well as a lower level of reactive power ripple (12.5%) in comparison to the PI control (14%). Using an LCL-filter in a grid-connected inverter is widely recognized to enhance harmonic and voltage regulation as compared to an L-filtered inverter. Nevertheless, LCL-filtered inverters exhibit greater complexity in both their design and application. Further investigation into the implementation of an LCL-filter could serve as a subject for future research in relation to the proposed control method.

2. Inverter Modeling

The attributes of the grid-connected inverter seen in Fig. 1. can be described as follows [29], [30] using Kirchoff's law at the pole voltage in each phase:

$$(L_f + L_g)\frac{di_a(t)}{dt} = v_{an}(t) - (R_f + R_g)i_a(t) - e_a(t) \tag{1}$$

$$(L_f + L_g)\frac{di_b(t)}{dt} = v_{bn}(t) - (R_f + R_g)i_b(t) - e_b(t) \tag{2}$$

$$(L_f + L_g)\frac{di_c(t)}{dt} = v_{cn}(t) - (R_f + R_g)i_c(t) - e_c(t) \tag{3}$$

Where L_f denotes filter inductance of the inverter, R_f represents filter resistance of the inverter, $L_g$is grid impedance, R_g is grid resistance, e denotes grid voltage, i is grid current and pole voltage vector is denoted as $u := [v_{an}v_{bn}v_{cn}]^T$. The dynamics (1)–(3) can be converted to the dq-frame model [31] as:

$$\frac{di(t)}{dt} = \tilde{A}i(t) + \tilde{B}u(t) + \tilde{E}(t) \tag{4}$$

Where

$$L = L_f + L_g \tag{5}$$

$$R = R_f + R_g \tag{6}$$

$i(t) := \begin{bmatrix} i_d(t) \\ i_q(t) \end{bmatrix}$, $u(t) := \begin{bmatrix} u_d(t) \\ u_q(t) \end{bmatrix}$, $\tilde{A} := \begin{bmatrix} -RL^{-1} & -\omega \\ \omega & -RL^{-1} \end{bmatrix}$, $\tilde{B} := \begin{bmatrix} L^{-1} & 0 \\ 0 & L^{-1} \end{bmatrix}$, and $\tilde{E}(t) := \begin{bmatrix} e_d(t) \\ e_q(t) \end{bmatrix}$.

Then, the continuous-time dynamic (4) can be converted into discrete time model [32]-[34] with the sampling instance *t* as:

$$i(k+1) = Ai(k) + Bu(k) + E(k) \tag{7}$$

where $A = I_2 + t\tilde{A}$, $B = t\tilde{B}$, $E = t\tilde{E}$, and I_2 is a second order identity matrix.

The design objective of a robust control is to withstand a worst-case scenario [35], such as uncertainty of the system. Therefore, the uncertainty of this system can be considered as a potential range of the filter's and grid's impedance. The uncertainties exist due to the rapid fluctuations in grid impedance during a failure or termination of a transmission line, as well as the impact of changes in operating temperature on the filter's impedance. The range is determined as follows [36], [37].

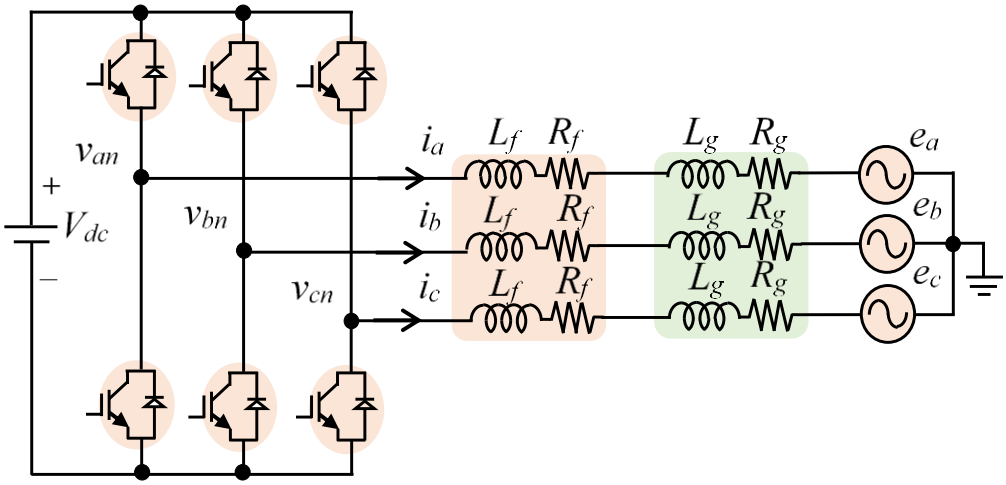

Fig. 1. Grid-connected inverter with grid impedance

$$Lf_{f,max}{}_{f,min} \tag{8}$$

$$Rf_{f,max}{}_{f,min} \tag{9}$$

$$Lg_{g,max}{}_{g,min} \tag{10}$$

$$Rg_{g,max}{}_{g,min} \tag{11}$$

Denoting the matrices pair of (A, B) corresponding to the sixteen possible combinations as (A_i, B_i) where ($i = 1, 2, \ldots, 16$). Then, the uncertainty model [38]-[40] of this grid-connected inverter can be formulated as bellows.

$$\Lambda = \left\{ \sum_{n=1}^{16} \gamma_n (A_i, B_i) \middle| \sum_{n=1}^{16} \gamma_n = 1, \gamma_n \geq 0 \right\} \tag{12}$$

The value of the lower and upper bounce of the parameters is defined as:

$$L_f/\gamma < L_f < \gamma L_f \tag{13}$$

$$R_f/\gamma < R_f < \gamma R_f \tag{14}$$

$$L_g/\gamma < L_g < \gamma L_g \tag{15}$$

$$R_g/\gamma < R_g < \gamma R_g \tag{16}$$

where($\gamma > 1$).

3. Robust Control Design

In the presence of grid voltage disturbance and inverter parameter change, the state feedback control normally fails to keep track of the reference state [41]. Thus, an integral control is employed to guarantee the stable and resilient performance of the proposed system. This proposed controller consists of integral to mitigate the steady-state error and state feedback control to provide stability to the system. The controller [42]-[44] is defined as:

$$\begin{cases} m(k) = m(k+1) + [i^* - i(k)] \\ u(k) = Fi(k) + Im(k) \end{cases} \tag{17}$$

where m is integral components, i^* denotes reference vector, u is the control input, F and I represent the state feedback and integral gain, respectively. The computing of gain F and I is done using a linear matrix inequality method. LMI-based optimization is a powerful tool used in various engineering and mathematical applications to efficiently solve complex optimization problems. By formulating the problem as a set of LMIs, this method allows for the use of convex optimization techniques to find the optimal solution. In order to regulate the output power, the current reference should be determined corresponding to the power reference P_{ref} with the elimination of reactive power. Therefore, the reference state is shown as follows [45].

$$i^* := \begin{bmatrix} i_d^* \\ i_q^* \end{bmatrix} = \frac{2P_{ref}}{3(e_d^2 + e_q^2)} \begin{bmatrix} e_d \\ e_q \end{bmatrix} \tag{18}$$

In case of regulating both active and reactive power, the reference can be defined as.

$$i^* := \frac{2P_{ref}}{3(e_d^2 + e_q^2)} \begin{bmatrix} e_d & -e_q \\ e_q & e_d \end{bmatrix} \begin{bmatrix} P_{ref} \\ Q_{ref} \end{bmatrix} \tag{19}$$

Subsequently, the system states and integral components can be augmented as:

$$h(k+1) = \bar{A}h(k) + \bar{B}u(k) + \bar{E}(k) \tag{20}$$

Where $h := \begin{bmatrix} i \\ m \end{bmatrix}$, $\bar{A} := \begin{bmatrix} A & 0_{2\times2} \\ I_2 & I_2 \end{bmatrix}$, $\bar{B} := \begin{bmatrix} B \\ 0_{2\times2} \end{bmatrix}$, $\bar{E} := \begin{bmatrix} E \\ i^* \end{bmatrix}$, and $0_{2\times2}$is two by two zero matrix. The closed-loop control input u is defined as

$$u(k) = Gh(k)\ (G := [FI]). \tag{21}$$

Then, from (17) and (20) the overall closed-loop system can be obtained assuming that the matrix $\bar{E}$ = 0 as

$$h(k+1) = (\bar{A} + \bar{B}G)h(k) \tag{22}$$

By applying the Lyapunov stability [46] condition to (22) representing the closed-loop dynamics, it is evident that:

$$(\bar{A} + \bar{B}G)^T \Theta (\bar{A} + \bar{B}G) - \Theta < -(1 - \lambda^2)\Theta \tag{23}$$

Here, $\lambda(0 < \lambda < 1)$ denotes the rate of convergence and Θ denotes a positive definite matrix. Next, utilizing the Schur's complement on (23) to obtain the linear matrix inequality representation:

$$\begin{bmatrix} \lambda^2\Theta & (\bar{A}+\bar{B}G)^T \\ \bar{A}+\bar{B}G & \Theta^{-1} \end{bmatrix} > 0 \tag{24}$$

The augmented closed-loop system (22) is stable if the inequality (24) holds [47] and it can be rewritten as.

$$\begin{bmatrix} \lambda^2\Psi & (\bar{A}\Psi+\bar{B}\Gamma)^T \\ \bar{A}\Psi+\bar{B}\Gamma & \Psi \end{bmatrix} > 0 \tag{25}$$

where $\Psi := \Theta^{-1}$, G is a stabilizing gain set, and $\Gamma = G\Psi$. Considering the sixteen possible uncertain sets of matrices pair $(A, B) \in \Lambda$in (12) to guarantee that the condition is satisfied at every corner of the set Λ, the LMI (25) can be redefined as:

$$\begin{bmatrix} \lambda^2\Psi & (\bar{A}_i\Psi+\bar{B}_i\Gamma)^T \\ \bar{A}_i\Psi+\bar{B}_i\Gamma & \Psi \end{bmatrix} > 0 \tag{26}$$

where $\bar{A}_i := \begin{bmatrix} A_i & 0_{2\times2} \\ I_2 & I_2 \end{bmatrix}$, $\bar{B}_i := \begin{bmatrix} B_i \\ 0_{2\times2} \end{bmatrix}$, ($i$ = 1, 2, 3, …, 16).

To shorten the convergence time [46] of the output voltage to the steady state which increasing the eigen value of the closed-loop system, λ should be selected with respect to the minimizing of Ψ under the LMI terms (26). Then, the optimization problem can be defined as.

$$\underset{\lambda,\Gamma}{Minimize}\ \Psi \quad \text{subject to (26)} \tag{27}$$

The controller derived by solving equation (27) ensures the fulfillment of the monotonicity criterion, hence guaranteeing overall stability in the presence of variations on parameters L_f, R_f, L_g and R_g within the specified range (8)–(11). Then, the optimal gain [48]-[50] can be obtained as.

$$G = \Gamma\Psi^{-1} \tag{28}$$

To efficiently solve this LMI problem a MATLAB toolbox called YALMIP [51] is used to compute the optimal gain. The YALMIP toolbox can be obtained by downloading it from [52]. The website includes comprehensive step-by-step instructions and a tutorial on how to solve this optimization problem using MATLAB. The control architecture of this proposed robust control can be found in Fig. 2.

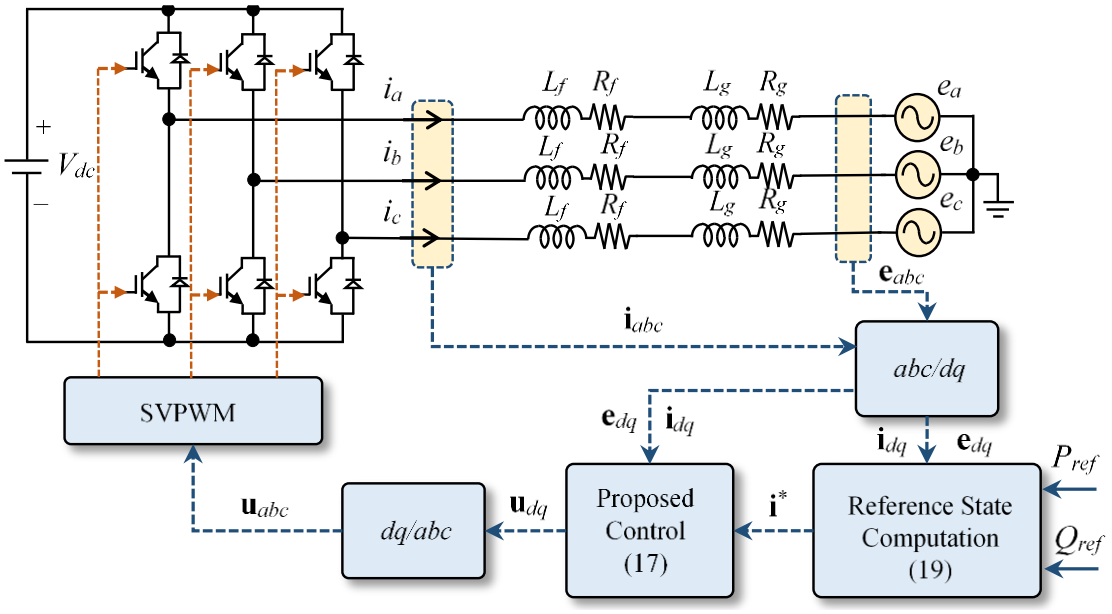

Fig. 2. Proposed robust control for a three-phase grid-connected inverter

4. Result and Discussions

The simulation study of this paper is done using MATLAB to compute the optimal gain with help from YALMIPS toolbox. Then the computed robust gain is used in the implementation of the control algorithm in PSIM. The simulation parameter is shown in Table 1. The parameters of this proposed system is chosen according to existed study of a grid-connected inverter [34] with additional grid impedance studied in [53]. The sample time is selected as 100 ms, resulting in a switching frequency of 10 kHz. Grid-connected inverters often employ a frequency of 10 kHz in order to limit the overall level of harmonic distortion. The summarized steps of the implementation of the control algorithm are presented Fig. 3.

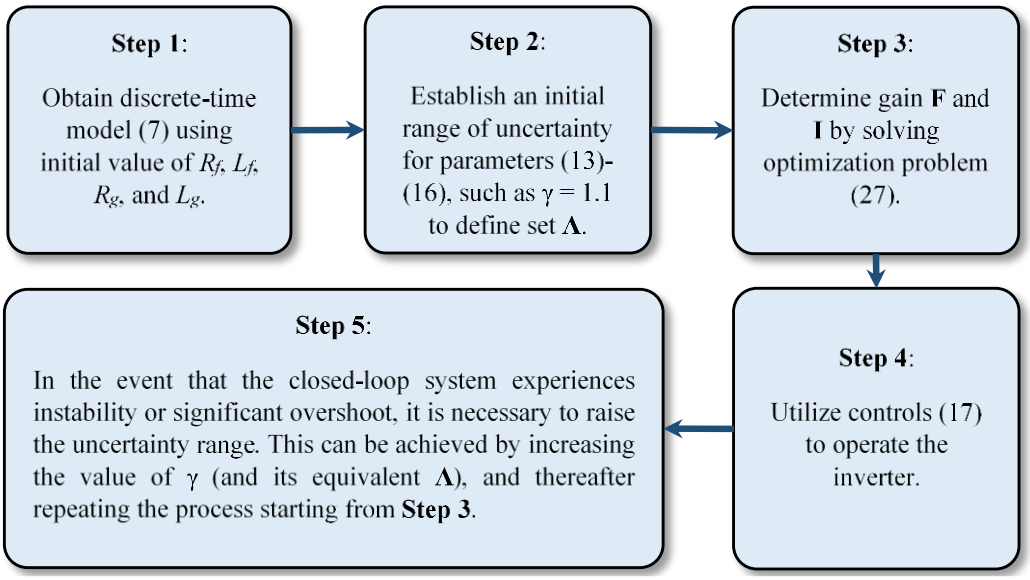

Fig. 3. Implementation step of this proposed control

Fig. 4 displays the current performance across several uncertainty ranges (γ = 1.1, 1.5, 2.4, and 3.0). In this scenario, the range of uncertainty can be regarded as a parameter for fine-tuning performance. It can be seen that the fastest output current with no overshoot can be obtained using γ = 1.5 in Fig. 4. The output becomes more sluggish when the value of γ rises. Thus, it is worth noting wider range results in a broader stability level with robustness to the disturbance of grid voltage, whereas a narrower range leads to improved speed of performance. Furthermore, the set of gains determined using four distinct forms of uncertainty range γ was implemented on the system using nominal values as indicated in Table 1.

Fig. 5 displays the closed-loop poles of the system. It is evident that regardless of the different ranges of γ, the poles of this proposed inverter remain within the stability range by staying within the complex unit circle. The poles of the closed-loop system (22) are derived from the computed gain G within several ranges of γ, specifically 1.1, 1.5, 2.4, and 3.3. Table 2 presents the eigenvalues corresponding to these ranges. It is important to mention that when the closed-loop poles lie on the complex unit circle, the overall system is marginally stable. However, if the poles are located outside the unit circle, the system becomes unstable. As the closed-loop poles move closer to the origin, the system's oscillations decrease.

Table 1. Proposed inverter's parameters

Parameter	Notations	Value
Filter inductance	L_f	3 mH
Filter resistance	R_f	0.1 Ω
Grid inductance	L_g	4.2 mH
Grid resistance	R_g	0.1 Ω
Grid voltage	$\mathbf{e}_{abc}$	310V(max)
Sampling Time	t	100 μs

Table 2. Closed-loop poles with different uncertainty ranges

γ = 1.1	γ = 1.5	γ = 2.4	γ = 3.3
0.8936 + 0.1090i	0.8626 + 0.0894i	0.8764 + 0.0137i	0.8966 + 0.0140i
0.8936 - 0.1090i	0.8626 - 0.0894i	0.8764 - 0.0137i	0.8966 - 0.0140i
0.8948 + 0.0824i	0.8641 + 0.0632i	0.6745 + 0.0110i	0.5046 + 0.0078i
0.8948 - 0.0824i	0.8641 - 0.0632i	0.6745 - 0.0110i	0.5046 - 0.0078i

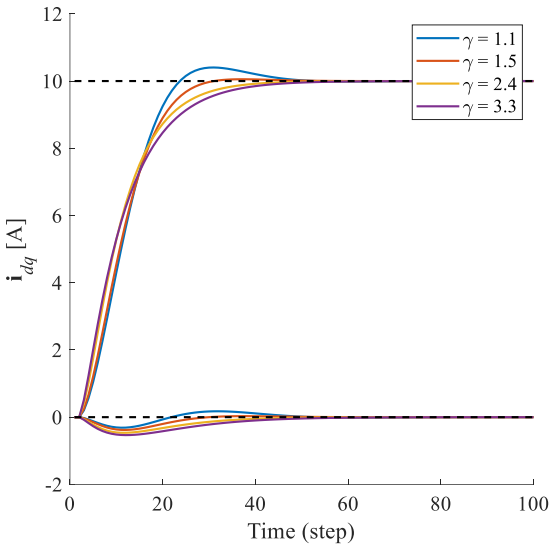

Fig. 4. the current output performance using different uncertainty bounce

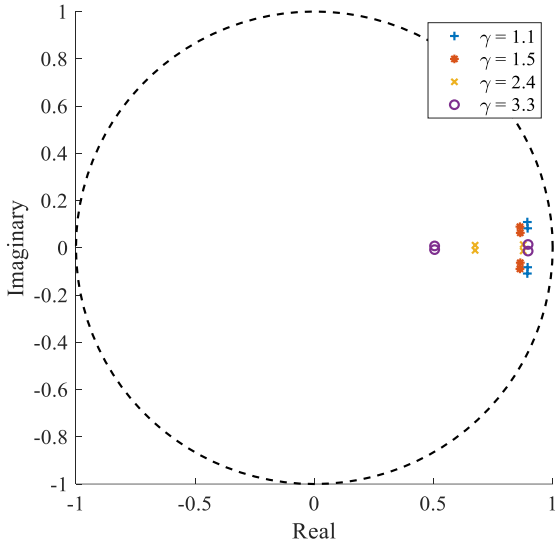

Fig. 5. closed-loop poles using different uncertainty bounces

In order to validate the robustness of this proposed inverter, the simulation is conducted by varying the parameter within the same uncertainty range, γ = 1.5. The controller in Fig. 6 is constructed using a nominal model that incorporates the nominal characteristics listed in Table 1. The active power reference is first set to 1000W at t = 0 and subsequently increases to 2000W at t = 0.1s. Throughout the whole simulation period, the reactive power reference remains at zero. The output power exhibits remarkably rapid transient characteristics, accompanied by exceptional and resilient tracking performance in the steady state. Fig. 7 and Fig. 8 depict the identical simulation procedure as Fig. 6, but with variations in the impedances of the filters and grid. Specifically, Fig. 7 uses impedances that are 25% higher than the nominal value, while Fig. 8 uses impedances that are 25% lower. Parameter values in the case of +25% and -25% variations can be found in Table 3. The results shows that the performance of this three cases are almost identical. It can be inferred that this proposed inverter exhibits robust performance regardless of parameter variations that are expected to occur in real-world settings.

Table 3. Parameter values in case of variations

Parameter	+25%	Nominal Value	–25%
L_f [mH]	3.750	3.000	2.250
R_f [Ω]	0.125	0.100	0.750
L_g [mH]	5.250	4.200	3.150
R_g [Ω]	0.100	0.100	0.750

Fig. 9 displays the operational efficiency of the three-phase inverter when regulating both active and reactive power. The active power reference is initially set to 2000W at t = 0.05s, and then decreases to zero at t = 0.15s. Similarly, the reactive power reference is initially set to 1000Var at t = 0.05s, and then decreases to zero at t = 0.1s. Both active and reactive power can be simultaneously controlled with quick transient performance.

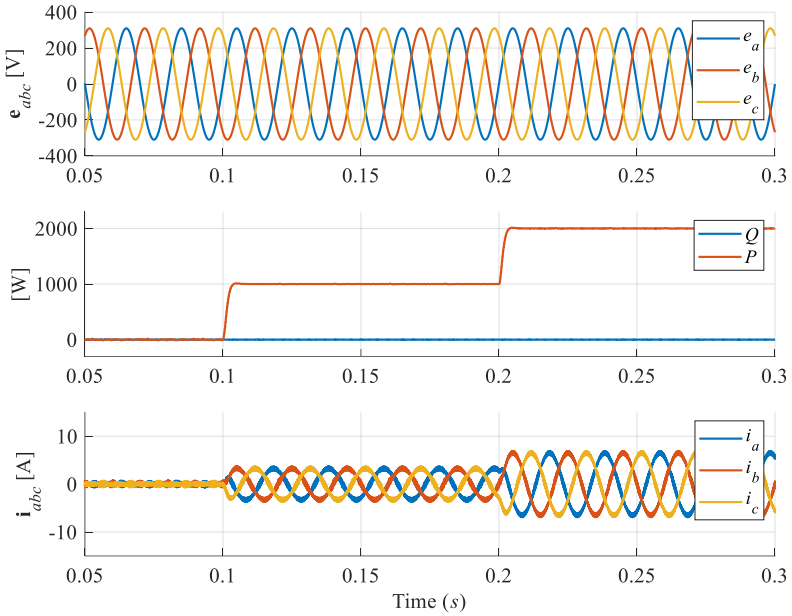

Fig. 6. from top to bottom, grid voltage, active and reactive power, grid current using uncertainty range γ = 1.5 under nominal parameter

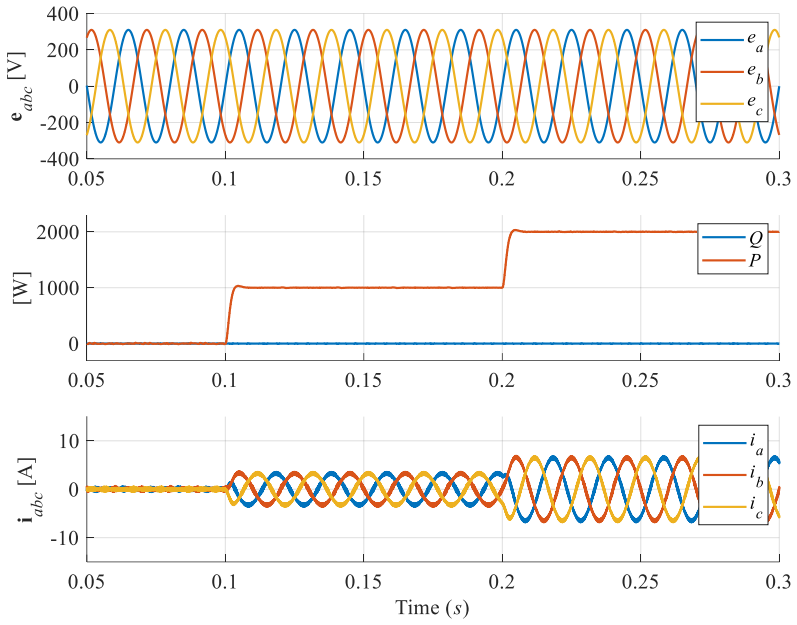

Fig. 7. From top to bottom, grid voltage, active and reactive power, grid current using uncertainty range γ = 1.5 under 25% increasing of the parameter

In order to confirm the efficacy of this proposed inverter control, the output active and reactive power were compared to those of the PI control under identical circumstances. To establish a fair comparison, the performance of PI control was manually tuned until the transient response showed similar levels of performance. In addition, an evaluation of the performance of these two controllers does not consider the transient power output, as the PI controller is not an optimal control strategy. Fig. 10 exhibits the comparison of output active power between the proposed control and PI control, both with a reference value of 2000 W. The picture is magnified to observe the level of ripple in both controllers and facilitate a fair comparison. The PI controller exhibits a ripple power of roughly 145W, whereas the proposed robust control has a ripple power of 25W. This corresponds to a ripple factor of 7.25% and 1.25% respectively. This demonstrates a notable enhancement with the

implementation of the proposed robust control. Fig. 11 shows a comparison of reactive power. It is evident that the PI control results in a ripple power of 140Var, while the proposed control has a ripple power of 125Var. This corresponds to a ripple factor of 14% and 12.5%, respectively. Similarly, the proposed control offers slightly improved performance. It is important to mention that the PI control does not require any modeling or step-by-step gain computation. This can be regarded as superior to the proposed control method, as it minimizes the need for modeling and gain computing procedures. However, the proposed control significantly improves the output power because it takes into account the predetermined uncertainty in this method.

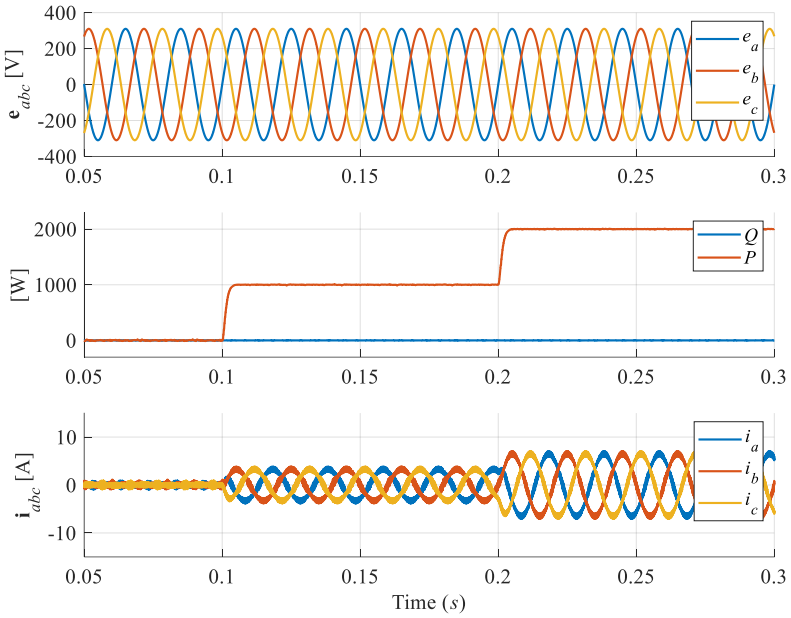

Fig. 8. from top to bottom, grid voltage, active and reactive power, grid current using uncertainty range γ = 1.5 under 25% decreasing of the parameter

The simulation results demonstrate that the proposed approach exhibits outstanding performance, even when there are fluctuations in the parameters of the inverter's filter and grid impedance. Furthermore, it offers a lower level of power ripple in comparison to PI control. Despite achieving a favorable outcome, there is still room for improvement in future iterations of this study. One potential enhancement is to incorporate the LCL-filter to more effectively reduce the total harmonic distortion (THD). Furthermore, this methodology can be enhanced from an economic standpoint by implementing grid voltage observers, thus obviating the necessity for voltage sensors in the experimental setup. To further evaluate the efficacy of this approach, an experiment can be conducted using an actual inverter system.

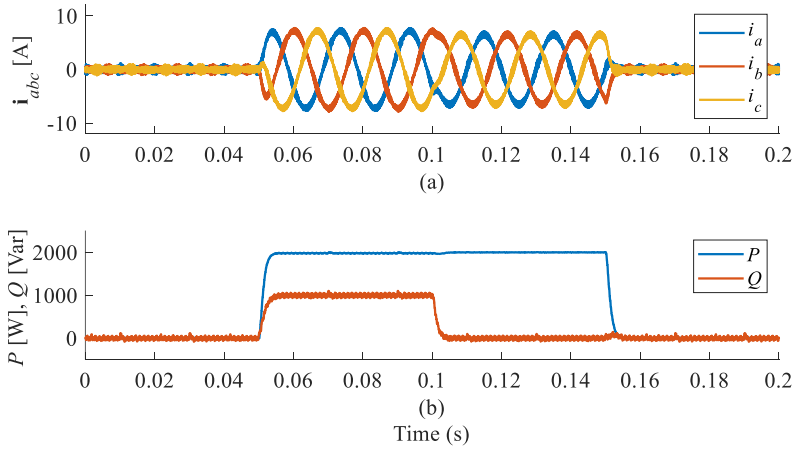

Fig. 9. Output power in case of regulating both active and reactive power

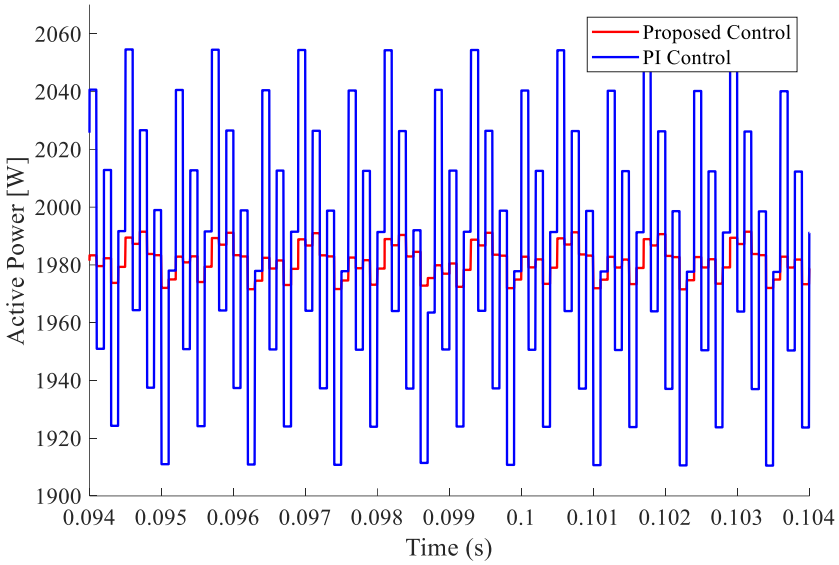

Fig. 10. Comparison of active power using the proposed control and PI control

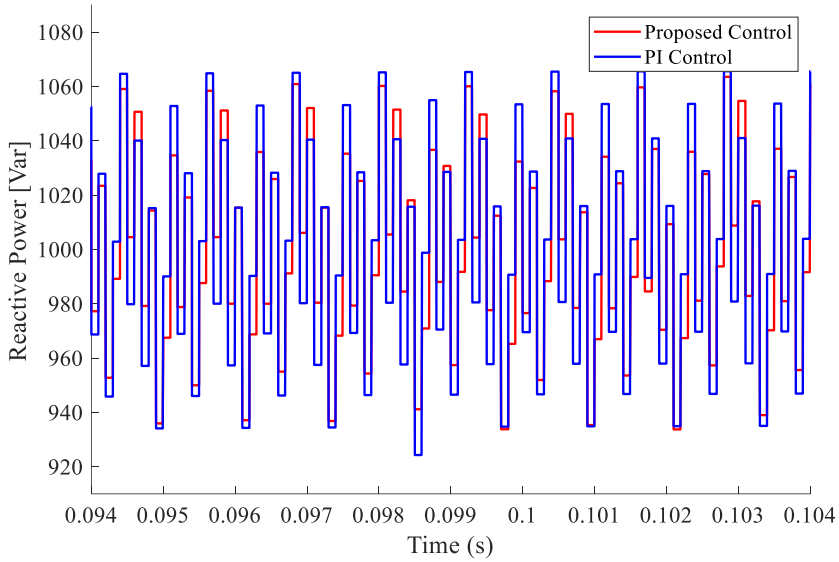

Fig. 11. Comparison of reactive power using the proposed control and PI control

5. Conclusion

The paper introduces a robust control design for a three-phase grid-connected inverter, taking into account uncertainties in both the system and the grid. Uncertain grid impedance is a problem that frequently occurs and can lead to voltage fluctuations, poor power quality, and possible device damage. This work provides a systematic control strategy to tackle these issues by supplying well-regulated power from a DC source to an AC power grid. With consideration of grid impedance in this paper, the control gain obtained by solving the LMI-based optimization problem ensures that the inverter operates well under variations in system and grid parameters. The simulation studies demonstrate that the inverter's output exhibits almost identical performance when subjected to parameter changes, even when employing nominal values of +25% and -25%.In addition, the simulation verifies that the proposed control demonstrates a reduced level of active power ripple (1.25%) compared to the PI control (7.25%), as well as a lower level of reactive power ripple (12.5%) compared to the PI control (14%).

Although the study has yielded a positive result, there is still potential for improvement in future works of this research. An option for improvement is to include the LCL-filter in order to improve

the THD of the output current. Moreover, grid voltage observers can economically enhance this approach by removing the need for voltage sensors in the experimental setup. In order to further determine the effectiveness and challenges of this method, it is advisable to carry out an experiment utilizing a real inverter system.

Author Contribution: All authors contributed equally to the main contributor to this paper. All authors read and approved the final paper.

Funding: This research received no external funding.

Acknowledgement: This research is supported by the National Polytechnic Institute of Cambodia.

Conflicts of Interest: The authors declare no conflict of interest.

References

[1] C. Choeung *et al*., "Linear Matrix Inequality-Based Optimal State Feedback Control of a Three-Phase L-filtered Grid-Connected Inverter," *2023 Third International Symposium on Instrumentation, Control, Artificial Intelligence, and Robotics (ICA-SYMP)*, pp. 135-139, 2023, https://doi.org/10.1109/ICA-SYMP56348.2023.10044932.

[2] P. Soth, S. San, H. Cheng, H. Tang, V. Torn and C. Choeung, "Voltage Regulation of a Three-Phase PV-Connected Inverter Using LMI-Based Optimization," *2023 International Conference on Advanced Mechatronics, Intelligent Manufacture and Industrial Automation (ICAMIMIA)*, pp. 1-5, 2023, https://doi.org/10.1109/ICAMIMIA60881.2023.10427886.

[3] G. Elhassan *et al*., "Deadbeat Current Control in Grid-Connected Inverters: A Comprehensive Discussion," *IEEE Access*, vol. 10, pp. 3990-4014, 2022, https://doi.org/10.1109/ACCESS.2021.3138789.

[4] Z. Wang, X. Sun, Y. Wu, and P. Yang, "Inverter Control Strategy Based on Improved Deadbeat Control and QPR Compound," *Journal of Physics: Conference Series*, vol. 1920, no. 1, p. 012038, 2021, https://doi.org/10.1088/1742-6596/1920/1/012038.

[5] V. R. Chowdhury and J. W. Kimball, "Adaptive Control of a Three-Phase Grid-Connected Inverter with near Deadbeat Response," *2021 IEEE Applied Power Electronics Conference and Exposition (APEC)*, pp. 2698-2701, 2021, https://doi.org/10.1109/APEC42165.2021.9486983.

[6] Z. Ju, X. Lv, B. Wu, L. Pu, W. Duan and P. Yang, "Advanced Model Predictive Control for Three-Phase Inverter Circuit Based on Disturbance Observer," *2019 IEEE 10th International Symposium on Power Electronics for Distributed Generation Systems (PEDG)*, pp. 900-904, 2019, https://doi.org/10.1109/PEDG.2019.8807605.

[7] J. Hong, B. Wang, X. Zhang, R. Cao, C. Xu and Z. Gao, "Improved Model Predictive Control Based on ADALINE algorithm," *2020 IEEE 9th International Power Electronics and Motion Control Conference (IPEMC2020-ECCE Asia)*, pp. 2697-2702, 2020, https://doi.org/10.1109/IPEMC-ECCEAsia48364.2020.9367643.

[8] S. Zhu, J. Huang, B. Wang, Y. Sun and X. Tong, "Event-Triggered Model Predictive Control of Three-phase Grid-connected Inverter with Operation State Consideration," *2020 Chinese Control And Decision Conference (CCDC)*, pp. 791-796, 2020, https://doi.org/10.1109/CCDC49329.2020.9164835.

[9] M. Azab, "High performance decoupled active and reactive power control for three-phase grid-tied inverters using model predictive control," *Protection and Control of Modern Power Systems*, vol. 6, no. 1, p. 25, 2021, https://doi.org/10.1186/s41601-021-00204-z.

[10] J. Jongudomkarn, "Multivariable Model Predictive Control for a Virtual Synchronous Generation-Based Current Source Inverter," *International Journal of Electrical and Electronic Engineering & Telecommunications*, vol. 10, no. 3, pp. 196-202, 2021, https://doi.org/10.18178/ijeetc.10.3.196-202.

[11] A. L. Julian and G. Oriti, "Novel Common Mode Voltage Elimination Methods in Three-Phase Four-Wire Grid-Connected Inverters," *2021 IEEE Energy Conversion Congress and Exposition (ECCE)*, pp. 2873-2880, 2021, https://doi.org/10.1109/ECCE47101.2021.9595958.

[12] L. Estrada, N. Vazquez, J. Vaquero, C. Hernandez, J. Arau and H. Huerta, "Finite Control Set – Model Predictive Control Based On Sliding Mode For Bidirectional Power Inverter," *IEEE Transactions on Energy Conversion*, vol. 36, no. 4, pp. 2814-2824, 2021, https://doi.org/10.1109/TEC.2021.3063601.

[13] T. Zhao, M. Zhang, C. Wang and Q. Sun, "Model-Free Predictive Current Control of Three-Level Grid-Connected Inverters With LCL Filters Based on Kalman Filter," *IEEE Access*, vol. 11, pp. 21631-21640, 2023, https://doi.org/10.1109/ACCESS.2023.3251410.

[14] W. Peng, Q. Chen, U. Manandhar, B. Wang and J. Rodriguez, "Event-Triggered Model Predictive Control for the Inverter of a Grid-Connected Microgrid With a Battery-Supercapacitor HESS," *IEEE Journal of Emerging and Selected Topics in Power Electronics*, vol. 11, no. 6, pp. 5540-5552, 2023, https://doi.org/10.1109/JESTPE.2022.3190306.

[15] E. Heydari and A. Y. Varjani, "Combined modified P&O algorithm with improved direct power control method applied to single-stage three-phase grid-connected PV system," *2018 9th Annual Power Electronics, Drives Systems and Technologies Conference (PEDSTC)*, pp. 347-351, 2018, https://doi.org/10.1109/PEDSTC.2018.8343821.

[16] M. Babaie, M. Mehrasa and K. Al-Haddad, "Direct Active and Reactive Power Control for Grid-Connected PEC9 Inverter Using Finite Control Set Model Predictive Method," *2021 22nd IEEE International Conference on Industrial Technology (ICIT)*, pp. 1371-1376, 2021, https://doi.org/10.1109/ICIT46573.2021.9453660.

[17] M. A. Djema, M. Boudour, K. Agbossou, A. Cardenas, and M. L. Doumbia, "GWO-based direct power control with improved LCL filter design for three-phase inverters," *International Journal of Digital Signals and Smart Systems*, vol. 5, no. 1, pp. 3-19, 2021, https://doi.org/10.1504/IJDSSS.2021.112791.

[18] F. T. Noori and T. K. Hassan, "Performance Comparison of Reactive Power Control Methods of Photovoltaic Micro-inverter," *Journal of Physics: Conference Series*, vol. 1973, no. 1, p. 012064, 2021, https://doi.org/10.1088/1742-6596/1973/1/012064.

[19] S. Dharmasena and A. I. Sarwat, "Fuzzy Decision Making Assisted Model Predictive Direct Power Controller for a Grid-Interlinking Converter of a Battery Energy Storage System," *2020 52nd North American Power Symposium (NAPS)*, pp. 1-6, 2021, https://doi.org/10.1109/NAPS50074.2021.9449778.

[20] C. Deng, Z. Shu, Y. Xia, N. Chen, T. Wang and H. Ma, "Three-phase photovoltaic grid-connected inverter with LCL based on current deadbeat control and PI control," *2014 International Conference on Power System Technology*, pp. 2864-2870, 2014, https://doi.org/10.1109/POWERCON.2014.6993846.

[21] M. Alathamneh, H. Ghanayem and R. M. Nelms, "Power Control of a Three-phase Grid-connected Inverter using a PI Controller under Unbalanced Conditions," *SoutheastCon 2022*, pp. 447-452, 2022, https://doi.org/10.1109/SoutheastCon48659.2022.9764097.

[22] Y. Wang, Z. Yan, Z. Zhang, H. Gu and Y. Gao, "A New PI Algorithm for Single Stage Three-Phase Grid-Connected Photovoltaic Inverter Based on Power Feed-Forward," *2015 Fifth International Conference on Instrumentation and Measurement, Computer, Communication and Control (IMCCC)*, pp. 1025-1030, 2015, https://doi.org/10.1109/IMCCC.2015.222.

[23] A. Chaithanakulwat, "Development of DC voltage control from wind turbines using proportions and integrals for three-phase grid-connected inverters," *International Journal of Electrical and Computer Engineering*, vol. 10, no. 2, pp. 1701-1711, 2020, https://doi.org/10.11591/ijece.v10i2.pp1701-1711.

[24] T. -F. Wu, Y. -H. Huang and Y. -T. Liu, "3Φ4W Grid-Connected Hybrid-Frequency Parallel Inverter System With Ripple Compensation to Achieve Fast Response and Low Current Distortion," *IEEE Transactions on Industrial Electronics*, vol. 68, no. 11, pp. 10890-10901, 2021, https://doi.org/10.1109/TIE.2020.3032920.

[25] Q. Zeng and L. Chang, "Study of advanced current control strategies for three-phase grid-connected pwm inverters for distributed generation," *Proceedings of 2005 IEEE Conference on Control Applications*, pp. 1311–1316, 2005, https://doi.org/10.1109/CCA.2005.1507313.

[26] H. Zhang, H. Zhou, J. Ren, W. Liu, S. Ruan, and Y. Gao, "Three-phase grid-connected photovoltaic system with SVPWM current controller," *2009 IEEE 6th International Power Electronics and Motion Control Conference*, pp. 2161-2164, 2009, https://doi.org/10.1109/IPEMC.2009.5157759.

[27] S. Bella *et al*., "Circulating Currents Control for Parallel Grid-Connected Three-Phase Inverters," *2018 International Conference on Electrical Sciences and Technologies in Maghreb (CISTEM)*, pp. 1-5, 2018, https://doi.org/10.1109/CISTEM.2018.8613377.

[28] M. F. Roslan, A. Q. Al-Shetwi, M. A. Hannan, P. J. Ker, and A. W. M. Zuhdi, "Particle swarm optimization algorithm-based PI inverter controller for a grid-connected PV system," *PLoS ONE*, vol. 15, no. 12, p. e0243581, 2021, https://doi.org/10.1371/journal.pone.0243581.

[29] H. Liao, X. Zhang and Z. Ma, "Robust dichotomy solution-based model predictive control for the grid-connected inverters with disturbance observer," *CES Transactions on Electrical Machines and Systems*, vol. 5, no. 2, pp. 81-89, 2021, https://doi.org/10.30941/CESTEMS.2021.00011.

[30] N. Mohammed, W. Zhou and B. Bahrani, "Comparison of PLL-Based and PLL-Less Control Strategies for Grid-Following Inverters Considering Time and Frequency Domain Analysis," *IEEE Access*, vol. 10, pp. 80518-80538, 2022, https://doi.org/10.1109/ACCESS.2022.3195494

[31] P. Soth *et al*., "Robust Dual-Current Control of a Three-Phase Grid-Tied Inverter under Unbalanced Grid Voltage Using LMI Approach," *2023 International Electrical Engineering Congress (iEECON)*, pp. 6-11, 2023, https://doi.org/10.1109/iEECON56657.2023.10126574.

[32] C. Choeung, M. L. Kry, and Y. I. Lee, "Robust Tracking Control of a Three-phase Charger under Unbalanced Grid Condition," *IFAC-PapersOnLine*, vol. 51, no. 28, pp. 173-178, 2018, https://doi.org/10.1016/j.ifacol.2018.11.697.

[33] V. Huy, H. Tang, P. Soth, S. Yay, K. Sovan and C. Choeung, "Three-phase Inverter using Robust Tracking Control based Interpolation," *2023 Third International Symposium on Instrumentation, Control, Artificial Intelligence, and Robotics (ICA-SYMP)*, pp. 91-95, 2023, https://doi.org/10.1109/ICA-SYMP56348.2023.10044739.

[34] C. Choeung, P. Soth, H. Tang, S. Ean, and S. Srang, "A Linear Matrix Inequality Approach to Optimal Voltage Control of a Three-Phase UPS Inverter under Unbalanced Loads," *Engineering Proceedings*, vol. 56, no. 1, p. 87, 2023, https://doi.org/10.3390/ASEC2023-15365.

[35] S. Li, J. Yang, W.-H. Chen, and X. Chen, "Disturbance Observer-Based Control," *Methods and Applications*, p. 340, 2016, https://doi.org/10.1201/b16570.

[36] I. R. Fitri, J. Kim, and H. Song, "A Robust Suboptimal Current Control of an Interlink Converter for a Hybrid AC/DC Microgrid," *Energies*, vol. 11, no. 6, p. 1382, 2018, https://doi.org/10.3390/en11061382.

[37] Y. Danayiyen, K. Lee, M. Choi, and Y. I. Lee, "Model Predictive Control of Uninterruptible Power Supply with Robust Disturbance Observer," *Energies*, vol. 12, no. 15, p. 2871, 2019, https://doi.org/10.3390/en12152871.

[38] J. S. Lim, J.-S. Kim, and Y. I. Lee, "Robust tracking model predictive control for input-constrained uncertain linear time invariant systems," *International Journal of Control*, vol. 87, no. 1, pp. 120-130, 2014, https://doi.org/10.1080/00207179.2013.823669.

[39] J. Kim and Y. I. Lee, "An Interpolation Technique for Input Constrained Robust Stabilization," *International Journal of Control, Automation and Systems*, vol. 16, pp. 1569–1576, 2018, https://doi.org/10.1007/s12555-017-0203-2.

[40] J. S. Lim and Y. I. Lee, "Design of a robust controller for three-phase UPS systems using LMI approach," *International Symposium on Power Electronics Power Electronics, Electrical Drives, Automation and Motion*, pp. 654–657, 2012, https://doi.org/10.1109/SPEEDAM.2012.6264527.

[41] S. Yoon, N. B. Lai, and K. Kim, "A Systematic Controller Design for a Grid-Connected Inverter with LCL Filter Using a Discrete-Time Integral State Feedback Control and State Observer," *Energies*, vol. 11, no. 2, p. 437, 2018, https://doi.org/10.3390/en11020437.

[42] H. Tang *et al*., "Design of a Robust Control for a Single-Phase AC-DC Converter Using LMI Technique," *2023 International Electrical Engineering Congress (iEECON)*, pp. 1-5, 2023, https://doi.org/10.1109/iEECON56657.2023.10126791.

[43] H. Tang, B. So, S. In, P. Soth, S. Yay and C. Choeung, "Single-Phase UPS Inverter Using Offset-Free Optimizing Control with Digital All-Pass Filter," *2023 International Conference on Advanced Mechatronics, Intelligent Manufacture and Industrial Automation (ICAMIMIA)*, pp. 156-160, 2023, https://doi.org/10.1109/ICAMIMIA60881.2023.10427840.

[44] C. Choeung, M. L. Kry, and Y. I. Lee, "Robust Tracking Control of a Three-Phase Charger under Unbalanced Grid Conditions," *Energies*, vol. 11, no. 12, p. 3389, 2018, https://doi.org/10.3390/en11123389.

[45] C. Choeung, M. L. Kry, and Y. I. Lee, "Robust Tracking Control of a Three-Phase Bidirectional Charger for Electric Vehicle," *Journal of Advanced Transportation*, vol. 2022, 2022, https://doi.org/10.1155/2022/5077091.

[46] J. S. Lim, C. Park, J. Han and Y. I. Lee, "Robust Tracking Control of a Three-Phase DC–AC Inverter for UPS Applications," *IEEE Transactions on Industrial Electronics*, vol. 61, no. 8, pp. 4142-4151, 2014, https://doi.org/10.1109/TIE.2013.2284155.

[47] S. Boyd, L. El Ghaoui, E. Feron, and V. Balakrishnan, "Linear Matrix Inequalities in System and Control Theory," *Society for Industrial and Applied Mathematics*, 1994, https://doi.org/10.1137/1.9781611970777.

[48] C. Choeung, H. Tang, P. Soth, V. Huy, and S. Srang, "LMI-Based Robust Voltage Regulation of a Single-Phase Inverter with LC-Filtered Output," *Computational Intelligence Methods for Green Technology and Sustainable Development*, vol. 567, pp. 314–324, 2022, https://doi.org/10.1007/978-3-031-19694-2_28.

[49] N. -B. Lai and K. -H. Kim, "Robust Control Scheme for Three-Phase Grid-Connected Inverters With LCL-Filter Under Unbalanced and Distorted Grid Conditions," *IEEE Transactions on Energy Conversion*, vol. 33, no. 2, pp. 506-515, 2018, https://doi.org/10.1109/TEC.2017.2757042.

[50] C. Choeung, S. H. Park, B. K. Koh, and Y. I. Lee, "Robust Tracking Control of a Three-Phase DC-AC Inverter for UPS Application under Unbalanced Load Conditions," *IFAC-PapersOnLine*, vol. 49, no. 27, pp. 278–283, 2016, https://doi.org/10.1016/j.ifacol.2016.10.704.

[51] J. Lofberg, "YALMIP: a toolbox for modeling and optimization in MATLAB," *2004 IEEE International Conference on Robotics and Automation (IEEE Cat. No.04CH37508)*, pp. 284-289, 2004, https://doi.org/10.1109/CACSD.2004.1393890.

[52] A. K. Ravat, A. Dhawan, M. Tiwari, "LMI and YALMIP: Modeling and optimization toolbox in MATLAB," *Advances in VLSI, Communication, and Signal* Processing, vol. 683, pp. 507-515, 2021, https://doi.org/10.1007/978-981-15-6840-4_41.

[53] S. -D. Kim, T. V. Tran, S. -J. Yoon, and K. -H. Kim, "Current Controller Design of Grid-Connected Inverter with Incomplete Observation Considering L-/LC-Type Grid Impedance," *Energies*, vol. 17, no. 8, p. 1855, 2024, https://doi.org/10.3390/en17081855.